Biosorption of cationic and anionic dyes using the biomass of *Aspergillus parasiticus* CBS 100926^T

Hadj Daoud Bouras, Ahmed RédaYeddou, Noureddine Bouras, Abdelmalek Chergui, Lidia Favier, Abdeltif Amrane and Nadir Dizge

ABSTRACT

Aspergillus parasiticus (*A. parasiticus*) CBS 100926^T was used as a biosorbent for the removal of Methylene Blue (MB), Congo Red (CR), Sudan Black (SB), Malachite Green Oxalate (MGO), Basic Fuchsin (BF) and Phenol Red (PR) from aqueous solutions. The batch biosorption studies were carried out as a function of dye concentration and contact time. The biosorption process followed the pseudo-first-order and the pseudo-second-order kinetic models and the Freundlich and Langmuir isotherm models. The resulting biosorbent was characterized by Scanning Electron Microscopy (SEM), X-Ray Diffractometer and Fourier Transformer Infrared Spectroscopy (FTIR) techniques. The results of the present investigation suggest that *A. parasiticus* can be used as an environmentally benign and low cost biomaterial for the removal of basic and acid dyes from aqueous solution.

Key words | Biosorption, *Aspergillus parasiticus*, dye, kinetics, isotherms modelling

HIGHLIGHTS

- Micro-fungi *Aspergillus parasiticus* CBS100926^T was employed as a new biosorbent for the biosorption of six dyes.
- The maximum dye capacity was found to be 131.58 mg/g.
- Adsorption processes can reach equilibrium within 120 min.
- Adsorption processes follow the pseudo-second-order rate equation.
- The results of equilibrium sorption were described through Langmuir and Freundlich isotherms.

Hadj Daoud Bouras (corresponding author)
Ahmed RédaYeddou
Abdelmalek Chergui
Laboratoire d'Etude et de Développement des Techniques de Traitement et d'Epuration des Eaux et de Gestion Environnementale (LEDTEGE),
Ecole Normale Supérieure de Kouba,
Vieux-Kouba, Alger,
Algeria
E-mail: *hadjdaoud_bouras@yahoo.fr*

Hadj Daoud Bouras
Département de Physique,
Ecole Normale Supérieure de Laghouat,
Laghouat,
Algeria

Noureddine Bouras
Laboratoire de Biologie des Systèmes Microbiens (LBSM),
Ecole Normale Supérieure de Kouba,
BP 92, 16308, Vieux-Kouba, Alger,
Algeria
and
Département de Biologie, Faculté des Sciences de la Nature et de la Vie et Sciences de la Terre,
Université de Ghardaia,
Ghardaïa 47000,
Algeria

Lidia Favier
Abdeltif Amrane
Univ-Rennes, Ecole Nationale Supérieure de Chimie de Rennes, CNRS, ISCR – UMR6226,
Rennes,
France

Nadir Dizge
Department of Environmental Engineering,
Mersin University,
Mersin, 33343,
Turkey

doi: 10.2166/wst.2021.005

GRAPHICAL ABSTRACT

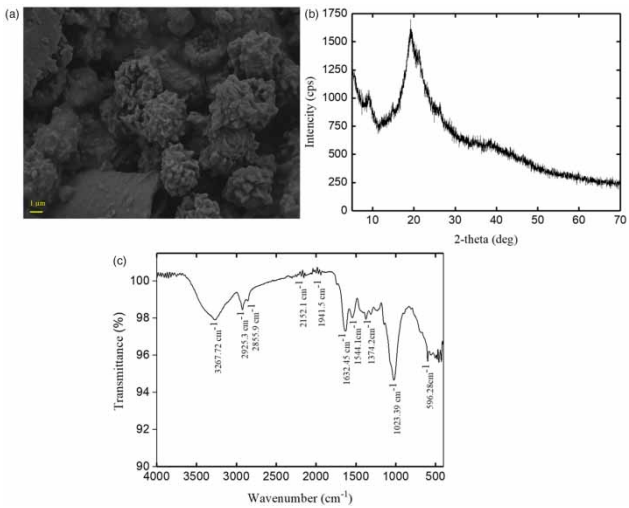

INTRODUCTION

Pigments and dyes, which have complex aromatic structures, are used widely in many areas such as paper, textile, food, cosmetic, leather, plastic and pharmaceutical industries (Bentahar *et al.* 2017). Various chemical dyes and large amounts of water are utilized to produce different products in the textile industry (Huang *et al.* 2016). The high costs involved in removing trace amounts of impurities make the search for appropriate treatment technologies an important priority (Arunarani *et al.* 2013). At this point, conventional approaches include biological treatment, coagulation, flocculation, ion exchange, membrane filtration and advanced oxidation processes; they are applicable for removal of synthetic dyes from industrial effluents (San *et al.* 2014; Moussa *et al.* 2017; Arikan *et al.* 2019; Bouras *et al.* 2019; Isik *et al.* 2019). Among all these techniques, biosorption is considered as one of the popular and attractive technologies for the removal of dyes from aqueous effluents when compared with the above processes (Raval *et al.* 2016). In this context, fungi and bacteria are broadly used for dye removal, such *as Aspergillus carbonarius* (Bouras *et al.* 2017), *Penicillium* YW01 (Yang *et al.* 2011), *Saccharomyces cerevisiae* (Ghaedi *et al.* 2013), *Pseudomonas putida* (Ghaedi & Vafaei 2017) and *Pseudomonas* sp. SUK1 (Kalyani *et al.* 2009).

The present work aims to investigate the biosorption capacity of *Aspergillus parasiticus* CBS 100926^T (AP) to remove six dyes: Methylene Blue (MB), Congo Red (CR), Sudan Black (SB), Malachite Green Oxalate (MGO), Basic Fuchsin (BF), and Phenol Red (PR) from aqueous solutions. The effects of some operating variables including dyes' concentration and contact time on the dyes biosorption were investigated in batch mode. Kinetic and isotherm analysis of the biosorption processes was analyzed in terms of the pseudo-first order, pseudo-second order models, Langmuir and Freundlich isotherm models, respectively. The characteristics of *Aspergillus parasiticus* biomass were evaluated by Scanning Electron Microscope (SEM) and Fourier Transform Infrared (FTIR) spectroscopy analysis.

MATERIALS AND METHODS

Preparation of the fungal biosorbent

The fungus *Aspergillus parasiticus* CBS100926^T (AP) was provided by the Center for Microbial Biotechnology, BioCentrum-DTU, Technical University of Denmark, DK-2800 Kgs. Lyngby, Denmark. *A. parasiticus* (AP) was grown in the liquid Sabouraud medium (10 g sucrose, 7 g peptone in 1 L of distilled water) at pH 6.8 and 25 °C. After 19 days of incubation (without shaking), the mycelial biomass was separated from the culture liquid Sabouraud medium by filtration, washed with ultrapure water and then

oven-dried at 80 ± 5 °C for 24 h. Dried biomass was crushed and sieved to 500 μm particle size using the ASTM standard test sieves (No: 35) to obtain homogenous size of AP biosorbent and then stored in glass bottles prior to use.

Preparation of stock solutions

The dyes used in this study were obtained from Sigma Aldrich with 99.99% purity. Stock solutions (100 mg/L) of MB, CR, SB, MGO, BF and PR were prepared in double distilled water and diluted to get the desired concentration of dyes. The characteristics of these dyes are listed in Table 1. The pH of the solutions was adjusted by addition of either 0.1 M HCl or 0.1 M NaOH solutions respectively.

Characterization of *Aspergillus parasiticus* biomass

The biosorbent was characterized by X-ray diffraction (XRD, Rigaku, Dmax-Rapid II) with an X-ray source of Cu Kα radiation ($\lambda = 1.5418$ Å). The scattering angle (2θ) was scanned from 5° to 70° at a scanning speed of 5°/min. The X-ray tube voltage and current were fixed at 40 kV and 30 mA, respectively. The Fourier transform infrared spectroscopy (FT-IR) analysis was done using Universal ATR Sampling Accessory with MIR detector and SPECTRUM Version 6.3.4 software from Perkin Elmer; it allowed investigation of the functional groups present on the biosorbent surface of AP in the range of 400–4,000 cm^{-1}. The surface and textural morphology of the biosorbent was captured using Scanning Electron Microscopy (SEM) (Zeiss Supra 55, Germany). The images were taken by applying an electron beam having an acceleration voltage of 10.0 kV.

Batch biosorption experiments

The experiments were performed by interacting various concentrations of dye (5–75 mg/L) solutions with *A. parasiticus* (0.5 g/L) in a rotary shaker (New Brunswick Scientific Company, New Jersey, USA) at 30 °C and 250 rpm for 24 h to attain equilibrium. The samples were centrifuged at 16,000 *g* (12,000 rpm) for 10 min to separate the solid phase from the liquid phase. The dye concentration in the supernatant solution was determined at λ_{max} of each dye using a UV–vis spectrophotometer (JENWAY UV–vis 6705). The amount of the dye uptaken and percentage of removal of dye by the adsorbent were calculated by applying Equations (1) and (2), respectively:

$$q_e = \frac{(C_0 - C_e)V}{m} \tag{1}$$

$$Removal\% = \frac{(C_0 - C_e)}{C_0} \times 100 \tag{2}$$

where C_0 and C_e are the initial and equilibrium concentrations of dye mg/L, respectively; V is the volume of the dye solution (L), and m is the amount of biosorbent used (g).

Biosorption kinetics and isotherm modeling

The equilibrium and the kinetics of a sorption process provide more important data when evaluating a sorption process as a unit operation (Bouras *et al.* 2015). Therefore, the kinetic of the dyes' biosorption on *A. parasiticus* was investigated and interpreted by applying the pseudo-first-order (Equation (3)) and pseudo-second-order (Equation (4)) kinetic models (Daoud *et al.* 2019).

$$Log(q_e - q_t) = Logq_e - \frac{k_1}{2.303}t \tag{3}$$

$$\frac{t}{q_t} = \frac{1}{k_2 q_e^2} + \frac{t}{q_e} \tag{4}$$

where q_e and q_t are the biosorption capacities of biosorbent at equilibrium time (mg/g) and time t (min), respectively, k_1 is the first-order rate constant (min^{-1}), k_2 is the equilibrium rate constant of pseudo-second-order biosorption (g/mg min), q_t (mg/g) is the amount of biosorption after time t (min) and q_e is the amount of biosorption equilibrium (mg/g). Biosorption kinetics was investigated with initial dye concentration of 50 mg/L from (0–180 min) at 30 °C and 250 rpm. Before addition of the *A. parasiticus*, pH was adjusted to the optimum value for each dye.

The models of Langmuir and Freundlich are based on different hypotheses. For the Langmuir model, the assumptions are: (i) all sites are equivalent, (ii) the adsorbing surface possess homogeneity, (iii) monolayer coverage; that is, each molecule can hold at most one molecule of adsorbate, (iv) there exists dynamic equilibrium between the adsorbed and free adsorbate molecules, (v) there are no interactions between adsorbate molecules on neighboring sites. Freundlich adsorption isotherm is an empirical model with the following assumptions: (i) the surface

Table 1 | Chemical structures of dyes

Dye	Structure	M_w (g/mol)	λ_{max} (nm)
CR (Congo Red)	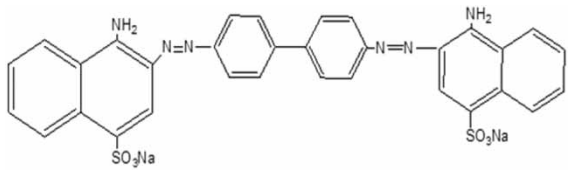	696.67	500
MB (Methylene Blue)	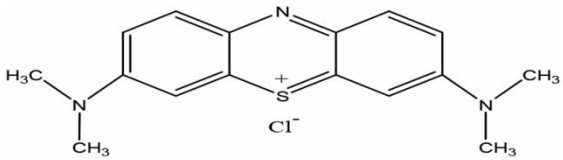	319.85	663
MGO (Malachite Green Oxalate)	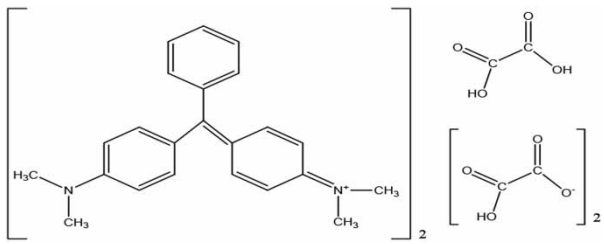	927.01	618
BF (Basic Fuchsin)	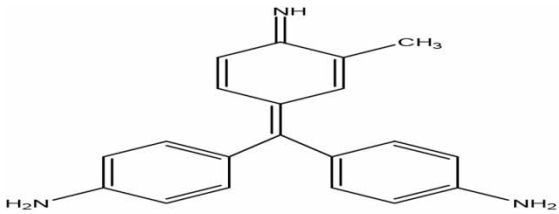	337.84	543
PR (Phenol Red)	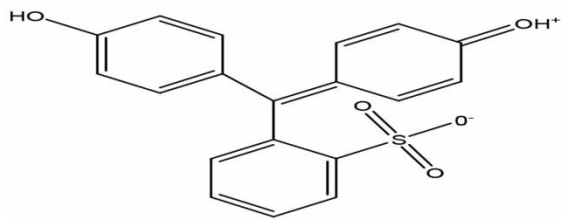	354.38	430
SB (Sudan Black)	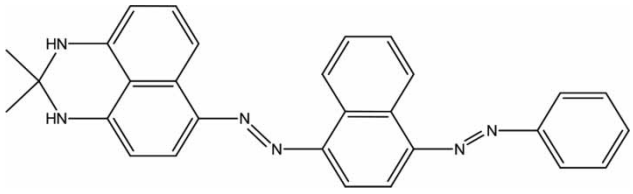	456.54	600

containing the adsorbing sites is heterogeneous, (ii) possibility of multi-layer adsorption, (iii) the active sites are non-uniform. However, in many works, the authors find that the coefficients of determinations are high and quite close for these two models. In order to evaluate the equilibrium data in our research, the Langmuir (Langmuir 1918) and Freundlich (Freundlich 1908) isotherm models (Equations (5) and (6)) were employed.

$$\frac{C_e}{q_e} = \frac{1}{q_{\max} k_L} + \frac{C_e}{q_{\max}} \tag{5}$$

$$Logq = \frac{1}{n} \log C_e + \log k_F \tag{6}$$

In Equation (5), q_{max} shows the maximum monolayer sorption capacity (mg/g), k_L is the Langmuir constant (L/mg), C_e is equilibrium dye concentration in the solution (mg/L) and q_e represents the amounts of dye sorbed onto the biosorbent at equilibrium (mg/g). In Equation (6), k_F represents the relative sorption capacity of biosorbent (L/g), n is a constant related to sorption intensity.

RESULTS AND DISCUSSION

Characteristics of *Aspergillus parasiticus* biomass

The SEM image of raw *A. parasiticus* is illustrated in Figure 1(a). The surface structure of the biosorbent material was uneven, heterogeneous, and porous. These irregular structures promote the trapping surface for uptake of dye solution (Bouras *et al.* 2020).

The XRD pattern of *A. parasiticus* is given in Figure 1(b). It was possible to identify a wide band in the 2θ range from 10° to 30°, which indicates that *A. parasiticus* biosorbent presented an amorphous structure. Similar behavior was found for diffraction patterns of other fungal biomasses (Drumm *et al.* 2019).

The FTIR spectrum of *A. parasiticus* is given in Figure 1(c). The main bands were at 3,267.72 cm^{-1}, which can be attributed to the stretching of O-H or N-H groups. The weak bands at 2,925.3 and 2,855.9 cm^{-1} can be ascribed to vibrations of the alkyl (C-H) groups. The bending vibration of hydroxyl group with asymmetric and symmetric stretching vibration of carboxyl groups (COOH) were acquired at 1,632.45, 1,544.1 and 1,374.2 cm^{-1}, respectively. The peak observed at 1,023.39 cm^{-1} was assigned to stretching vibration of C–O bands. Moreover, the band observed at 596.28 cm^{-1} for the biosorbent represented C–N–C scissoring that is only found in protein structures. Through this spectrum, it was possible to identify that the biomass of

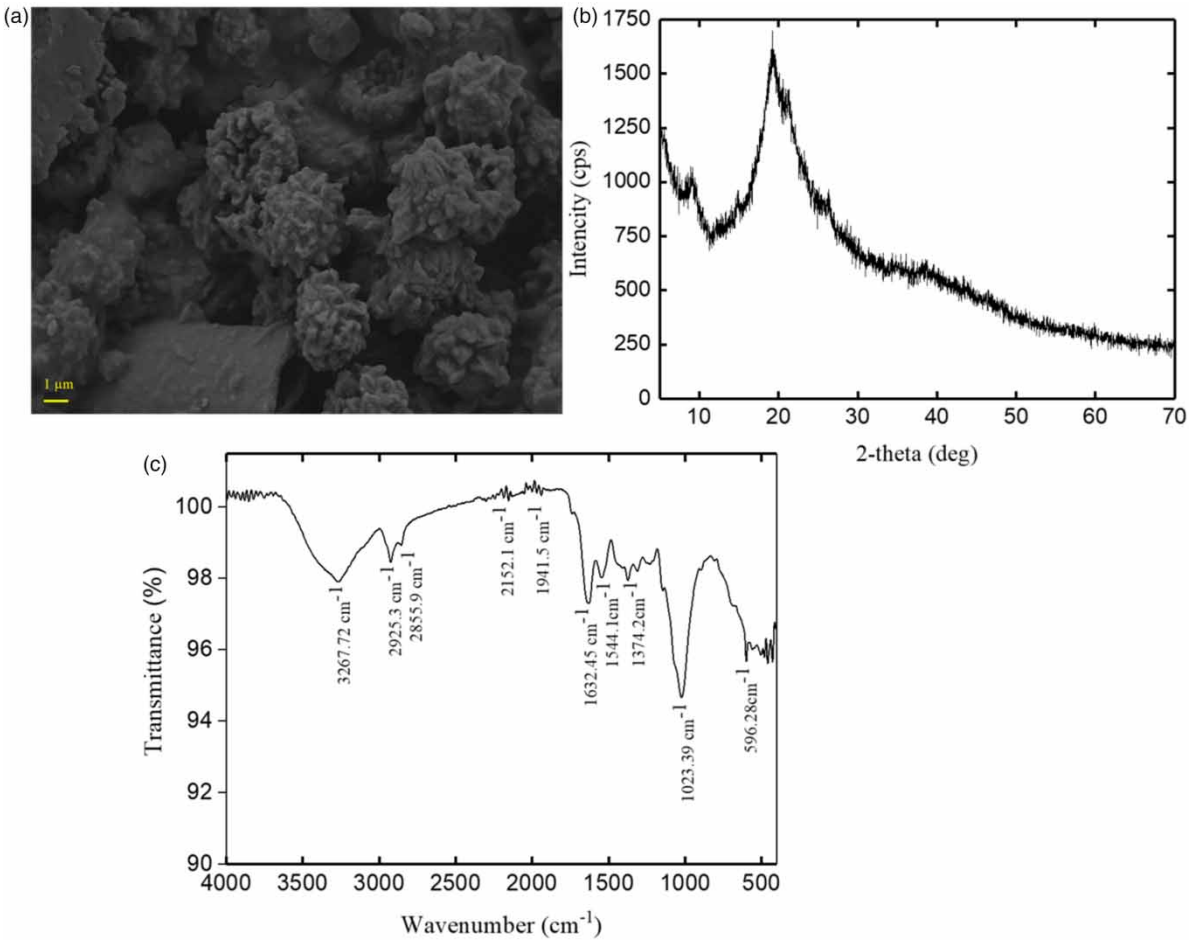

Figure 1 | (a) SEM image, (b) XRD pattern, and (c) FT-IR vibrational spectrum of *Aspergillus parasiticus* CBS 100926^T biomass.

the fungus *A. parasiticus* contains hydroxyl, amine, carboxyl and amide groups on its surface.

Effect of pH

The pH is the most important factor for adsorption studies, which affects not only the adsorption capacity, but also colour and the dye chemistry in the medium. The biosorption of these dyes was highly pH dependent and optimum values are shown in Table 2. A pH below 5 could be favourable for the biosorption between the CR and AP, because a significantly high electrostatic attraction could exist between the positively charged surface of *A. parasiticus* by absorbing H^+ ions and the anionic dyes. Whereas for PR dye, as the pH of the solution increased, the surface of the biosorbent became negatively charged, which decreased the biosorption of the negatively charged PR anions by electrostatic repulsive forces.

The optimum pH of the dyes BF and MB were 8 and 8.5, respectively. The adsorption process was maximum at basic pH for MB and BF, indicating that the negatively charged AP surface was responsible for the biosorption. Lower biosorption capacity of MGO observed at basic pH was a result of competition between the excess hydroxyl ions and the negatively charged dye ions for the biosorption sites. For increasing pH, the number of positively charged sites on *A. parasiticus* decreased and the number of negatively charged sites increased, part of the SB molecule exists as anions, and the adsorption was significantly impeded. Similar results of the effect of chemical structure of dyes were also reported (Sun *et al.* 2015; Dhananasekaran *et al.* 2016; Shoukat *et al.* 2017; Koyuncu & Kul 2020). The fungal mycelium did not release any adsorbed dyes. This observation revealed that the species has a greater chemical stability when subjected to adverse environmental conditions. For this reason, the chemical stability has the potential to act as an excellent candidate to bioremediate the solution dye.

Table 2 | Optimum conditions for biosorption of different dyes onto *Aspergillus parasiticus* CBS 100926^T

Dye	pH	Time (min)	C_{dye} (mol/L)	q (mg/g)
CR	4.5	60	7.2×10^{-5}	78.72
MB	8.5	60	1.6×10^{-4}	73.07
BF	8.0	60	1.0×10^{-4}	42.72
MGO	8.5	60	5.4×10^{-5}	35.00
SB	8	60	1.1×10^{-4}	24.29
PR	7.5	20	1.4×10^{-4}	06.25

Biosorption kinetic profiles

As shown in Figure 2, the biosorption capacity of the biomass was significantly high in the initial 60 min and thereafter gradually reached equilibrium within 120 min. The results are due to the fact that at the initial stage of the biosorption process, there was more availability and abundance of active sites on the surface of the biosorbent. After this time, these sites are occupied and the remaining vacant active biosorption sites decrease.

The kinetic constants and the values of R^2 are presented in Table 3. As presented in Table 3, the correlation coefficient values were high, from which it could be concluded that the pseudo-second-order model could well describe the biosorption kinetics and their calculated q_e values agreed well with the experimental q_e values.

Equilibrium modelling

The biosorption capacity for AP at different initial dye concentrations process is shown in Figure 3. The uptake amounts of dye increased with increasing initial dye concentrations up to 50 mg/L for CR, MB, BF, MGO, SB and to 30 mg/L for PR dyes, respectively it remained unchanged by further increase in initial dye concentrations. These results suggest that the available sites on the biosorbent are the limiting factor for dye biosorption.

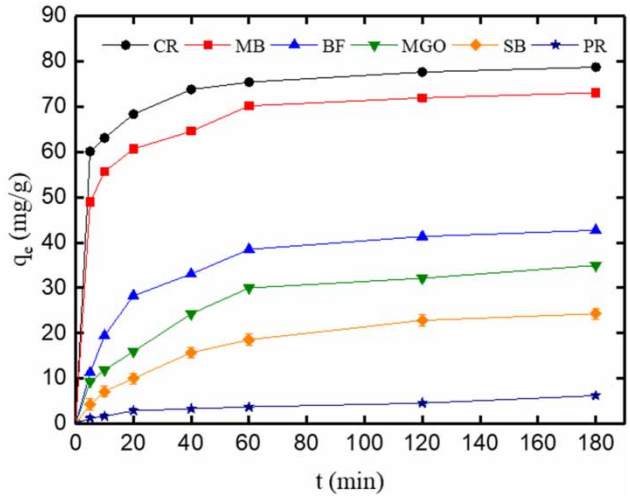

Figure 2 | Effect of contact time on biosorption of dyes onto *Aspergillus parasiticus* CBS 100926^T.

Table 3 | Kinetic biosorption parameters at 298 K

Model	CR	MB	BF	MGO	SB	PR
Kinetic						
$q_{e,\ exp}$ (mg/g)	78.72	73.07	42.72	35.00	24.29	6.25
Pseudo-first-order						
k_1 (1/min)	0.0569	0.0613	0.0615	0.0463	0.0525	0.0207
$q_{e1,cal}$ (mg/g)	17.49	22.41	28.47	25.73	22.05	04.59
R^2	0.908	0.978	0.970	0.891	0.901	0.980
Pseudo-second-order						
k_2 (g/mg.min)	0.0070	0.0050	0.0023	0.0020	0.0018	0.0153
$q_{e2,cal}$ (mg/g)	78.13	72.99	44.25	35.46	25.97	04.90
R^2	0.999	0.998	0.987	0.967	0.942	0.973

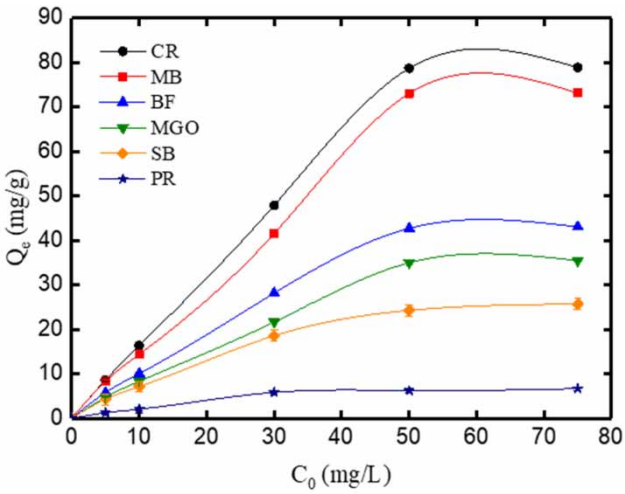

Figure 3 | Biosorption equilibrium isotherms of dyes onto *Aspergillus parasiticus* CBS 100926^T.

Table 4 | Isotherm parameters for the dyes' biosorption by the biomass *Aspergillus parasiticus* CBS 100926^T

	Aspergillus parasiticus					
Sample Dye	CR	MB	BF	MGO	SB	PR
Langmuir						
q_m (mg/g)	131.58	63.29	58.48	50.76	33.33	10.81
K_L (L/mg)	0.097	0.172	0.050	0.039	0.050	0.029
R^2	0.980	0.935	0.985	0.991	0.987	0.991
Freundlich						
K_F (mg/g) $(mg/L)^{1/n}$	12.48	9.52	3.64	2.51	2.34	0.53
n	1.62	1.56	1.47	1.42	1.61	1.57
R^2	0.909	0.926	0.963	0.974	0.971	0.943

Table 4 shows the adsorption isotherms and the predicted isothermal parameters, respectively. The biosorption isotherm data were characterized perfectly by the Langmuir isotherm model. Regarding the Freundlich isotherm, the value of the n constant, falling in the range of 1–10, also showed a suitable biosorption process (Deniz & Kepekci 2017). However, the values of correlation coefficients indicate that the data are not well correlated to the Freundlich model compared to the Langmuir correlation coefficients.

The considered biomass has not been previously tested as a biosorbent and hence there is a lack of literature data in view of comparison to the results of this study. However, Table 5 gives a comparison of the maximum adsorption capacity of *A. parasiticus* with recent studies of some other adsorbents reported in literature. According to the data presented in Table 5, in general the maximum biosorption capacity of dye onto *A. parasiticus* biomass is one of the highest among biomasses. Meanwhile, other materials in the literature showed high adsorption, as reported in many studies (Arabkhani & Asfaram 2019; Afshariani & Roosta 2019; Georgin *et al.* 2020). The availability and cost effectiveness of *Aspergillus parasiticus* could provide an inexpensive source of biosorbents for sequestering toxic dyes from industrial effluents.

CONCLUSION

In this study, pH, initial dye concentration and contact time were optimized for each dye. Biosorption of dye molecules by an adsorbent could be through electrostatic interaction,

Table 5 | Comparison of maximal adsorptive capacity (q_m) of the biomass of *Aspergillus parasiticus* CBS 100926^T

Biosorbents	pH	Dye	q_m (mg/g)	References
Aspergillus parasiticus 100926^T	8.2	MB	63.29	Present work
Crosslinked chitosan mushroom bio-composite	7.0	MB	40.11	Yildirim (2020)
Scenedesmus sp.	9.0	MB	87.69	Afshariani & Roosta (2019)
Aspergillus parasiticus 100926^T	4.5	CR	131.58	Present work
Antigonon leptopus	5.0	CR	18.18	Sri Devi *et al.* (2020)
Eichhornia crassipes	9.0	CR	05.18	Roy & Mondal (2019)
Aspergillus parasiticus 100926^T	8.0	BF	58.48	Present work
Powdered mandacaru leaves	8.0	BF	398.9	Georgin *et al.* (2020)
Eggshell membrane	6.0	BF	48	Bessashia *et al.* (2020)
Aspergillus parasiticus 100926^T	8.5	MGO	50.76	Present work
Three D MBCNF/GOPA	7.0	MG	270.27	Arabkhani & Asfaram (2019)
Lannea coromandelica	8.3	MG	50	Mate *et al.* (2020)
Aspergillus parasiticus 100926^T	8.0	SB	33.33	Present work
Aspergillus parasiticus 100926^T	7.5	PR	10.81	Present work

chemical binding or by a combination of all processes. The adsorption isotherm fitted well to the Langmuir model and the kinetics of adsorption fitted best to the pseudo-second-order model. The adsorption capacities of *Aspergillus parasiticus* for dye molecules vary according to the sequence: PR < SB < MGO < BF < MB < CR. The maximum biosorption capacity was 131.58 mg/g. Results indicate that *Aspergillus parasiticus* can provide an efficient and cost-effective technology for eliminating dyes from aqueous solution.

DATA AVAILABILITY STATEMENT

All relevant data are included in the paper or its Supplementary Information.

REFERENCES

Afshariani, F. & Roosta, A. 2019 Experimental study and mathematical modeling of biosorption of methylene blue from aqueous solution in a packed bed of microalgae *Scenedesmus*. *Journal of Cleaner Production* **225**, 133–142.

Arabkhani, P. & Asfaram, A. 2019 Development of a novel three-dimensional magnetic polymer aerogel as an efficient adsorbent for malachite green removal. *Journal of Hazardous Materials* **384**, 121394.

Arikan, E. B., Isik, Z., Bouras, H. D. & Dizge, N. 2019 Investigation of immobilized filamentous fungi for treatment of real textile industry wastewater using up flow packed bed bioreactor. *Bioresource Technology Reports* **7**, 100197.

Arunarani, A., Chandran, P., Ranganathan, B. V., Vasanthi, N. S. & Sudheer Khan, S. 2013 Bioremoval of Basic Violet 3 and Acid Blue 93 by *Pseudomonas putida* and its adsorption isotherms and kinetics. *Colloids and Surfaces B: Biointerfaces* **102**, 379–384.

Bentahar, S., Dbik, A., Khomri, M. E., Messaoudi, N. E. & Lacherai, A. 2017 Adsorption of methylene blue, crystal violet and Congo red from binary and ternary systems with natural clay: kinetic, isotherm, and thermodynamic. *Journal of Environmental Chemical Engineering* **5** (6), 5921–5932.

Bessashia, W., Berredjem, Y., Hattab, Z. & Bououdina, M. 2020 Removal of basic fuchsin from water by using mussel powdered eggshell membrane as novel bioadsorbent: equilibrium, kinetics, and thermodynamic studies. *Environmental Research* **186**, 109484.

Bouras, H. D., Benturki, O., Bouras, N., Attou, M., Donnot, A., Merlin, A., Addoun, F. & Holtz, M. D. 2015 The use of an agricultural waste material from *Ziziphus jujuba* as a novel adsorbent for humic acid removal from aqueous solutions. *Journal of Molecular Liquids* **211**, 1039–1046.

Bouras, H. D., Yeddou, A. R., Bouras, N., Hellel, D., Holtz, M. D., Sabaou, N., Chergui, A. & Nadjemi, B. 2017 Biosorption of Congo red dye by *Aspergillus carbonarius* M333 and *penicillium glabrum* Pg1: kinetics, equilibrium and thermodynamic studies. *Journal of the Taiwan Institute of Chemical Engineers* **80**, 915–923.

Bouras, H. D., Isik, Z., Arikan, E. B., Bouras, N., Chergui, A., Yatmaz, H. C. & Dizge, N. 2019 Photocatalytic oxidation of azo dye solutions by impregnation of ZnO on fungi. *Biochemical Engineering Journal* **146**, 150–159.

Bouras, H. D., Isik, Z., Arikan, E. B., Yeddou, A. R., Bouras, N., Chergui, A., Favier, L., Amrane, A. & Dizge, N. 2020 Biosorption characteristics of methylene blue dye by two fungal biomasses. *International Journal of Environmental Studies* doi:10.1080/00207233.2020.1745573.

Daoud, M., Benturki, O., Girods, P., Donnot, A. & Fontana, S. 2019 Adsorption ability of activated carbons from *Phoenix dactylifera* rachis and *Ziziphus jujube* stones for the removal of commercial dye and the treatment of dyestuff wastewater. *Microchemical Journal* **148**, 493–502.

Deniz, F. & Kepekci, R. A. 2017 Bioremoval of Malachite green from water sample by forestry waste mixture as potential biosorbent. *Microchemical Journal* **132**, 172–178.

Dhananasekaran, S., Palanivel, R. & Pappu, S. 2016 Adsorption of methylene blue, bromophenol blue and Coomassie Brilliant Blue by α-chitin nanoparticles. *Journal of Advanced Research* **7** (1), 113–124.

Drumm, F. C., Grassi, P., Georgin, J., Tonato, D., Pfingsten Franco, D. S., Chaves Neto, J. R., Mazutti, M. A., Jahn, S. L. & Dotto, G. L. 2019 Potentiality of the *Phoma* sp. inactive fungal biomass, a waste from the bioherbicide production, for the treatment of colored effluents. *Chemosphere* **235**, 596–605.

Freundlich, H. 1908 Uber die adsorption in losungen. *Zeitschrift fur Physikalische Chemie* **57** (A), 358–471.

Georgin, J., Franco, D., Drumm, F. C., Grassi, P., Netto, M. S., Allasia, D. & Dotto, G. L. 2020 Powdered biosorbent from the mandacaru cactus (*Cereus jamacaru*) for discontinuous and continuous removal of Basic Fuchsin from aqueous solutions. *Powder Technology* **364**, 584–592.

Ghaedi, A. M. & Vafaei, A. 2017 Applications of artificial neural networks for adsorption removal of dyes from aqueous solution: a review. *Advances in Colloid and Interface Science* **245**, 20–39.

Ghaedi, M., Hajati, S., Barazesh, B., Karimi, F. & Ghezelbash, G. 2013 *Saccharomyces cerevisiae* for the biosorption of basic dyes from binary component systems and the high order derivative spectrophotometric method for simultaneous analysis of Brilliant green and Methylene blue. *Journal of Industrial and Engineering Chemistry* **19**, 227–233.

Huang, J., Liu, D., Lu, J., Wang, H., Wei, X. & Liu, J. 2016 Biosorption of reactive black 5 by modified *Aspergillus versicolor* biomass: kinetics, capacity and mechanism studies. *Colloids and Surfaces A: Physicochemical and Engineering Aspects* **492** (5), 242–248.

Isik, Z., Arikan, E. B., Bouras, H. D. & Dizge, N. 2019 Bioactive ultrafiltration membrane manufactured from *Aspergillus carbonarius* M333 filamentous fungi for treatment of real textile wastewater. *Bioresource Technology Reports* **5**, 212–219.

Kalyani, D. C., Telke, A. A., Dhanve, R. S. & Jadhav, J. P. 2009 Ecofriendly biodegradation and detoxification of reactive Red 2 textile dye by newly isolated *Pseudomonas* sp. SUK1. *Journal of Hazardous Materials* **163**, 735–742.

Koyuncu, H. & Kul, A. R. 2020 Removal of methylene blue dye from aqueous solution by nonliving lichen (*Pseudevernia furfuracea* (L.) Zopf.), as a novel biosorbent. *Applied Water Science* **10**, 72.

Langmuir, I. 1918 The adsorption of gases on plane surfaces of glass, mica and platinum. *Journal of the American Chemical Society* **40** (9), 1361–1403.

Mate, C. J., Mishra, S. & Srivastava, P. K. 2020 Design of pH sensitive low-cost adsorbent from the exudate of *Lannea coromandelica* (Houtt) for remediation of Malachite Green dye from aqueous solution. *Polymer Bulletin* doi:10.1007/s00289-020-03263-8.

Moussa, D. T., El-Naas, M. H., Nasser, M. & Al-Marri, M. J. 2017 A comprehensive review of electrocoagulation for water treatment: potentials and challenges. *Journal of Environmental Management* **186**, 24–41.

Raval, N. P., Shah, P. U. & Shah, N. K. 2016 Malachite green 'a cationic dye' and its removal from aqueous solution by adsorption. *Applied Water Science* **7** (7), 3407–3445.

Roy, T. K. & Mondal, N. K. 2019 Potentiality of *Eichhornia* shoots ash towards removal of Congo red from aqueous solution: isotherms, kinetics, thermodynamics and optimization studies. *Groundwater for Sustainable Development* **6**, 100269.

San, N. O., Celebioglu, A., Tümtaş, Y., Uyar, T. & Tekinay, T. 2014 Reusable bacteria immobilized electrospun nanofibrous webs for decolorization of methylene blue dye in wastewater treatment. *RSC Advances* **4** (61), 32249–32255.

Shoukat, S., Bhatti, H. N., Iqbal, M. & Noreen, S. 2017 Mango stone biocomposite preparation and application for crystal violet adsorption: a mechanistic study. *Microporous and Mesoporous Materials* **239**, 180–189.

Sri Devi, V., Sudhakar, B., Prasad, K., Jeremiah Sunadh, P. & Krishna, M. 2020 Adsorption of Congo red from aqueous solution onto Antigonon leptopus leaf powder: equilibrium and kinetic modeling. *Materials Today: Proceedings* **26** (2), 3197–3206.

Sun, X., Ou, H., Miao, C. & Chen, L. 2015 Removal of Sudan dyes from aqueous solution by magnetic carbon nanotubes: equilibrium, kinetic and thermodynamic studies. *Journal of Industrial and Engineering Chemistry* **22**, 373–377.

Yang, Y., Jin, D., Wang, G., Liu, D., Jia, X. & Zhao, Y. 2011 Biosorption of acid blue 25 by unmodified and CPC-modified biomass of *Penicillium* YW01: kinetic study, equilibrium isotherm and FTIR analysis. *Colloids and Surfaces B: Biointerfaces* **88**, 521–526.

Yildirim, A. 2020 Kinetic, equilibrium and thermodynamic investigations for the bio-sorption of dyes onto crosslinked *Pleurotus ostreatus*-based bio-composite. *International Journal of Environmental Analytical Chemistry* doi:10.1080/03067319.2020.1802441.

First received 1 September 2020; accepted in revised form 18 December 2020. Available online 2 January 2021